



## Research article

# Homogenization heat treatment influence on microstructure evolution and mechanical properties of as-cast Al–Li–Cu–Mg–Zr alloy for lightweight aerospace application

Abdellah Lahbari<sup>a</sup>, Kenza Bouchaala<sup>a,\*</sup>, Hamza Essoussi<sup>b</sup>, Mustapha Faqir<sup>a</sup>, Said Ettaqi<sup>b</sup>, El Hachmi Essadiqi<sup>a</sup>

<sup>a</sup> International University of Rabat, School of Aerospace & Automotive Engineering, LERMA Lab, Sala El Jadida, Morocco

<sup>b</sup> Laboratory of Energy, Materials and Sustainable Development, ENSAM, Moulay Ismail University, 15290, Meknes, Morocco

## ARTICLE INFO

## Keywords:

Al–Li–Cu–Mg–Zr alloy  
Homogenization heat treatment  
Mechanical properties  
Microstructures  
Precipitates  
Microsegregation

## ABSTRACT

Al–Li–Cu–Mg–Zr alloys are widely used in the aerospace industry for different applications and make an excellent concurrent to high-performance composites. This family of alloys has remarkable properties like low density, high elastic modulus, high strength and specific stiffness, fracture toughness, fatigue crack growth resistance, and improved corrosion resistance.

The present work aims to investigate a family of Al–Li alloys by employing suitable characterization techniques such as computer-aided cooling curve analysis and thermal dilatometry to characterize the as-cast alloy. The characterization temperatures of the alloy were obtained and the phase transformation temperatures were concluded as thermal expansion inflection points as well. Furthermore, the homogenization heat treatment effect of the alloy is examined through optical microscopy (OM), scanning electron microscopy (SEM), Energy-dispersive X-ray spectroscopy (EDS), X-ray diffraction (XRD) and Vickers microhardness testing to determine the optimum heat treatment time. The results reveal the formation of  $\delta'$ ,  $\delta$  and  $\beta'$  precipitates in the alloy after different hours of homogenization heat treatment. Notably, our investigation identifies the optimum heat treatment time for the alloy as 26h at 515 °C, resulting in reduced hardness and barely any chemical segregation. These findings contribute to the characterization of as-cast Al–Li alloys and the understanding of microstructure evolution and mechanical properties during homogenization heat treatment that offer a valuable insight for enhancing their performance in aerospace applications.

## 1. Introduction

In recent decades, Al–Li alloys have gained a place in aerospace materials panoply as lightweight materials with relatively good mechanical properties [1]. These alloys have found applications in aircraft wings, space rocket oxygen tanks, and plane floor beams [2–4]. Binary Al–Li alloys exhibit a 6%–8% increase in elastic modulus while reducing density by 3% for every 1% addition of lithium [5,6]. To further enhance the alloy properties, the industrial Al–Li alloys are typically alloyed with the addition of several elements. Cu, Mg and Ag are added for solution strengthening and precipitate strengthening. Zn improves corrosion properties, while Zr and Mn

\* Corresponding author.

E-mail address: [kenza.bouchaala@uir.ac.ma](mailto:kenza.bouchaala@uir.ac.ma) (K. Bouchaala).

<https://doi.org/10.1016/j.heliyon.2024.e24426>

Received 3 August 2023; Received in revised form 12 December 2023; Accepted 9 January 2024

Available online 11 January 2024

2405-8440/© 2024 Published by Elsevier Ltd.

This is an open access article under the CC BY-NC-ND license

(<http://creativecommons.org/licenses/by-nc-nd/4.0/>).

**Table 1**  
Material chemical composition in weight.

Element	Li	Cu	Mg	Zr	Mn	Al
%	2.2–2.5	1.3–1.8	0.8	0.1	0.1	Bal.

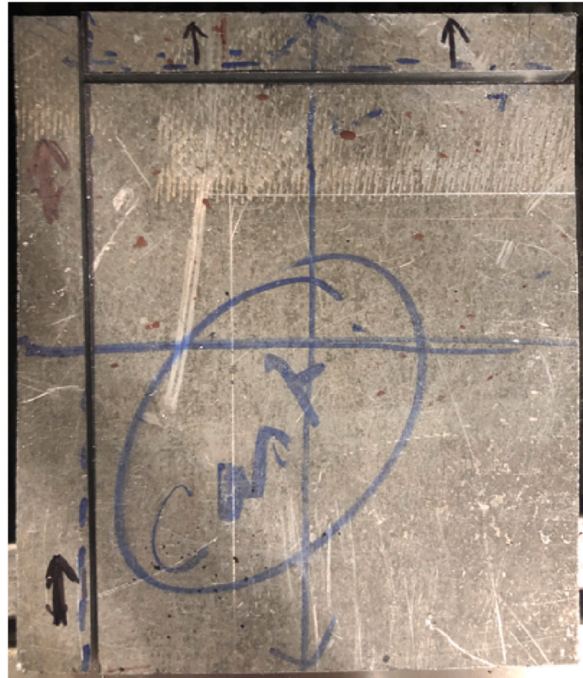


**Fig. 1.** As-cast ingot.

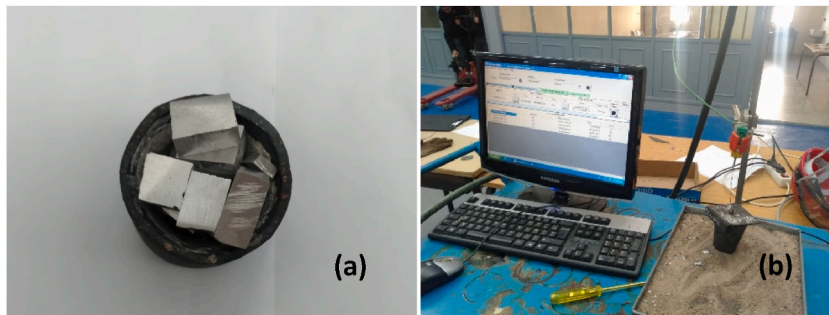


**Fig. 2.** Computer-aided cooling curve analysis (a) sample (b) experimental set-up.

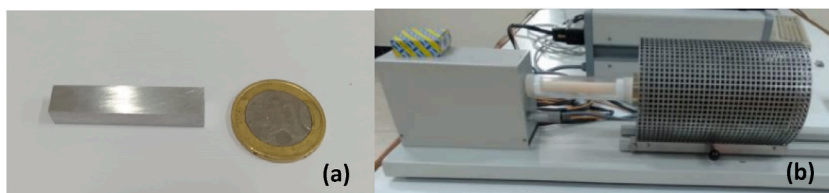


**Fig. 3.** Thermal dilatation analysis (a) sample (b) experimental set-up.



Fig. 4. Homogenization specimens in the furnace.

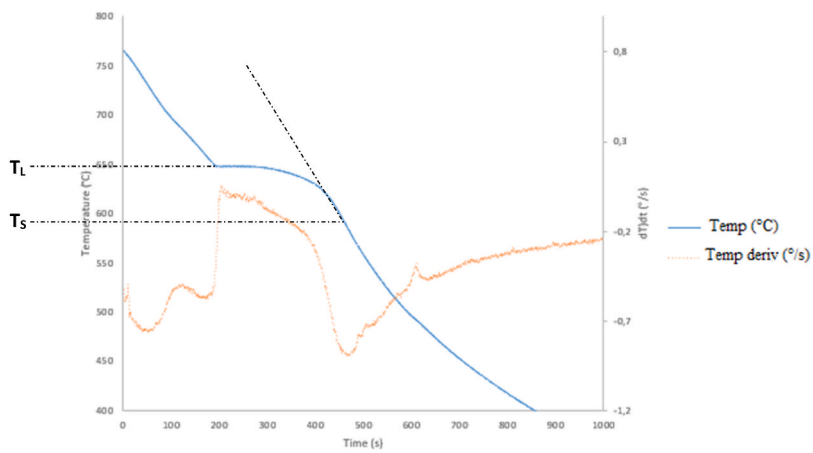


Fig. 5. Cooling curve and its derivative.

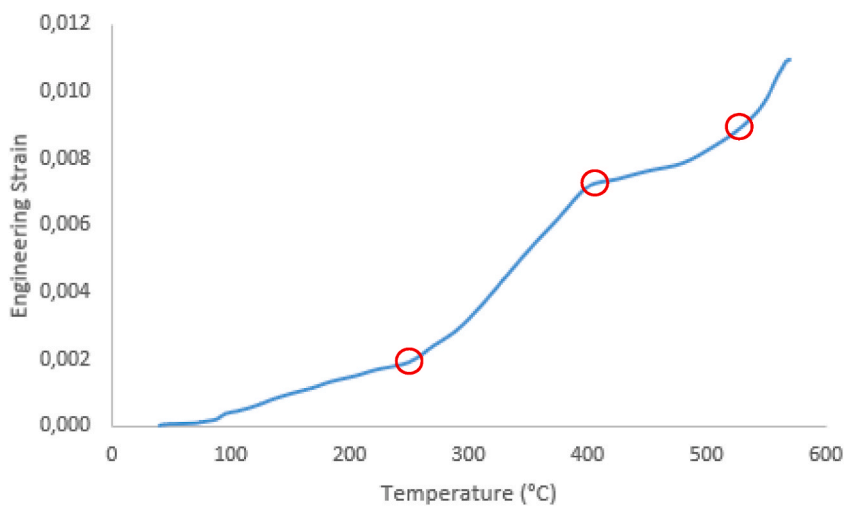
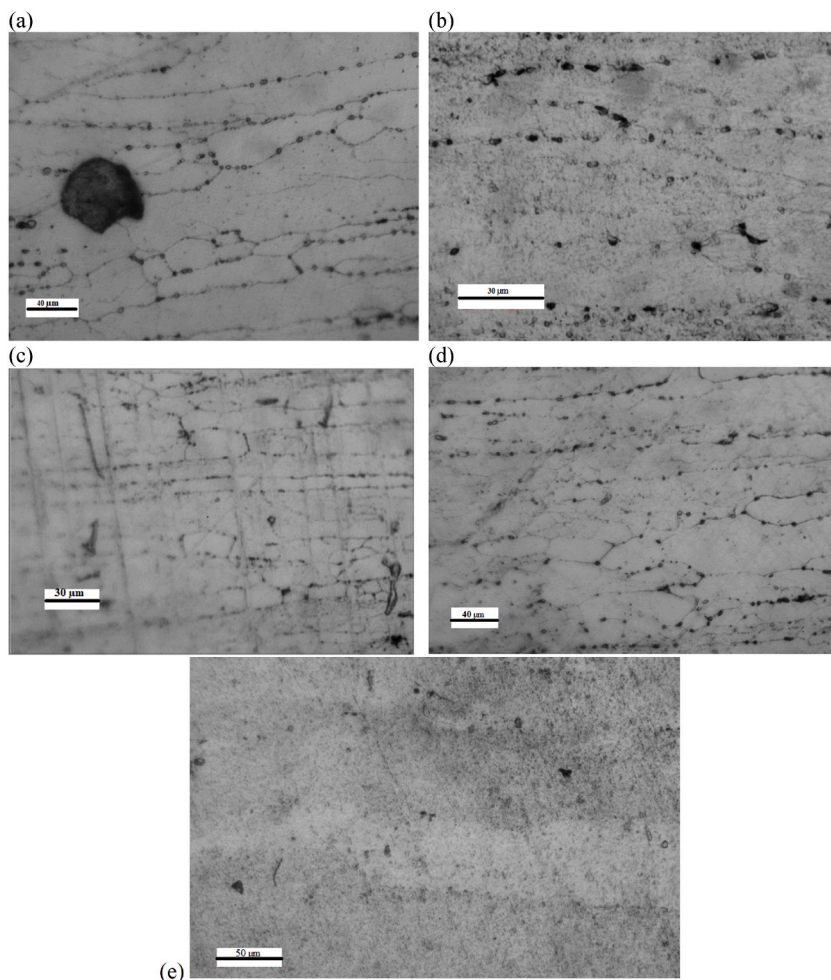


Fig. 6. Dilatometry curve.



**Fig. 7.** Optical microscope images, (a) 0h, (b) 16h, (c) 26h, (d) 38h and (e) 48h

contribute to texture control and govern the recrystallization process [7,8]. The precipitates in Al–Li alloys like  $\delta'$ (Al<sub>3</sub>Li), T<sub>1</sub>(Al<sub>2</sub>CuLi) and T<sub>B</sub>(Al<sub>7.5</sub>Cu<sub>4</sub>Li) are the milestone with regard to the material mechanical properties. The strengthening is ensured by the precipitates  $\delta'$ , T<sub>1</sub> and T<sub>2</sub>(Al<sub>6</sub>CuLi<sub>3</sub>) and S'(Al<sub>2</sub>CuMg). The precipitates T<sub>1</sub>, T<sub>2</sub> and T<sub>B</sub> contribute to the toughness of the alloy, whereas  $\beta'$  (Al<sub>3</sub>Zr) acts as a pin in the grain boundaries, regulating recrystallization and controlling texture [7,9].

The casted slabs of metals need homogenization heat treatment to avoid segregation and eliminate non-equilibrium eutectic phases. This heat treatment is conducted in 3 steps: heat-up, soak and cool down and it precedes generally high temperature forming like extrusion, hot forging or hot rolling [10]. This process leads to a more workable material with better uniformity of internal structure. Several studies have focused on investigating the as-cast and homogenized states of Al–Li alloys using various approaches. For instance, Wei et al. [11] studied a systematic homogenization heat treatment on an Al–Li–Cu–Mg–Zr alloy and found that the best combination was 530 °C for 24h, followed by air cooling. Rezaei et al. study [12] investigated the homogenization of an Al–1Li–3Cu–0.1Zr and Al–2Li–3Cu–0.1 Zr concluding that the heat treatment should be conducted at 500 °C for 24 h. Zhang et al. [13] examined the as-cast and homogenized AA2099 alloy, revealing the presence of a severe dendritic structure. They optimized the heat treatment process in a two-step approach (515 °C for 18h followed by 525 °C for 16h). A quasi-in-situ study [14] focused on the microstructural evolution of AA2195 and the observed results showed the precipitates T<sub>B</sub>, S and  $\theta$ (Al<sub>2</sub>Cu) at each temperature level. Li et al. [15] explored the homogenization process of AA2060 alloy and deduced that the optimum two-stage homogenization treatment of the studied alloy was 460 °C for 4h followed by 490 °C for 24h. Shengli et al. [16] investigated single-step and double-step homogenization for an Al–Cu–Li alloy determining that the optimum heat treatment schedule was 498 °C for 24h followed by 515 °C for 24h.

In the present paper, we aim to conduct a thermal analysis study on the as-cast alloy. Moreover, we will investigate the homogenization treatment of an Al–Li–Cu–Mg–Zr alloy to identify the optimal heat treatment before the rolling process. The outcomes of this research will contribute to the understanding of the behavior of Al–Li alloys and give valuable insight into its homogenization heat treatment.

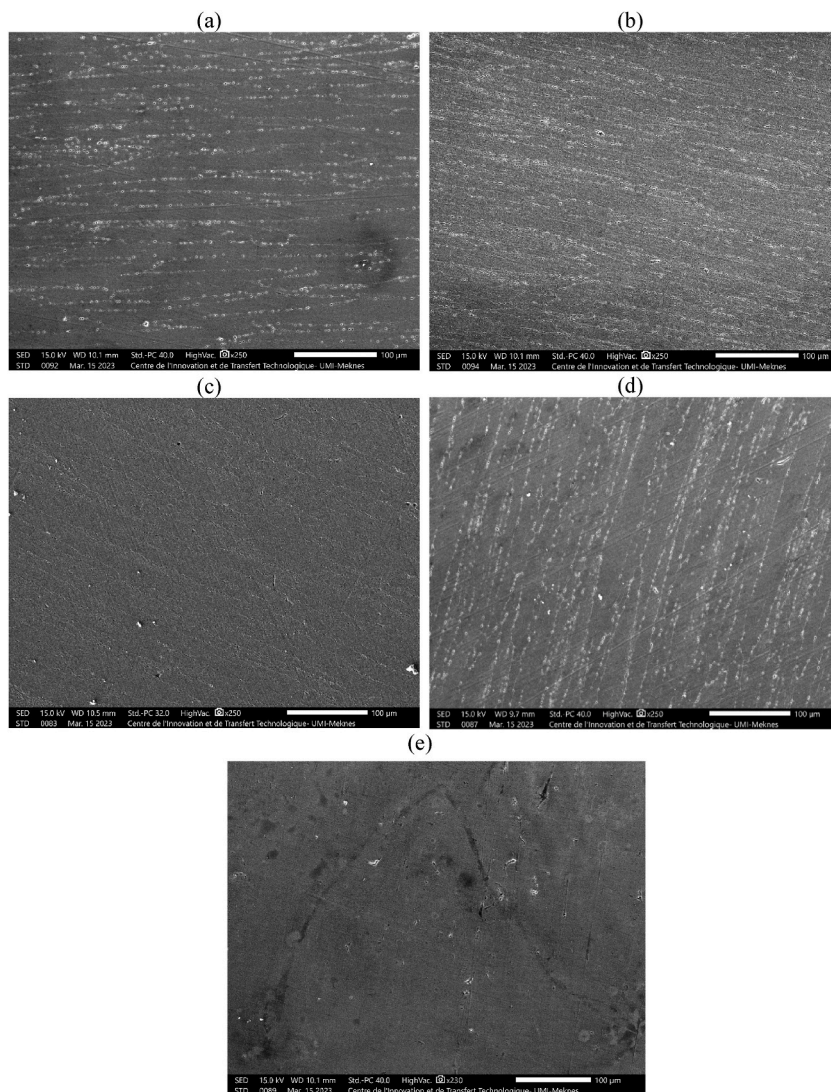


Fig. 8. SEM images (a) 0h, (b) 16h, (c) 26h, (d) 38h and (e) 48h

## 2. Material and experimental procedure

The studied material is an Al–Li–Cu–Mg–Zr alloy characterized by a density of  $2540 \text{ kg/m}^3$ . The detailed chemical composition of the alloy is presented in Table 1. Knowing the explosive nature of lithium metal especially at high temperatures, the ingots of the alloy were prepared utilizing a closed casting process [17,18]. The resulting as-cast ingot with the dimensions  $200 \times 200 \times 45 \text{ mm}^3$ , depicted in Fig. 1, serves as a starting point for subsequent investigations and analysis.

The as-cast alloy was characterized by two fundamental techniques: Thermal analysis of cooled sample and thermal dilatometry. In the thermal analysis technique, the alloy underwent controlled heating until it reached the molten state, followed by cooling in ambient air. The temperature evolution during cooling was recorded as a function of time using a computer-aided cooling curve analysis technique, enabling the determination of crucial thermal parameters (refer to Fig. 2(a and b)).

The second technique, dilatometry also known as thermal dilatation analysis, was employed to analyze the linear change of dimension of the specimen as a function of temperature. The dilatometry measurements were carried up to a temperature of  $570 \text{ }^\circ\text{C}$  as shown in Fig. 3(a and b). This technique provided the phase transformation temperatures as they present inflection points of the dilatometry curve.

For the investigation of homogenization heat treatment effects, the specimens were cut from near the center of the as-cast ingot and subjected to a series of homogenization heat treatments with respect to the following schedule: 0h (reference), 16h, 26h, 38h and 48h at a temperature of  $515 \text{ }^\circ\text{C}$  (Fig. 4). A comprehensive examination of the specimens was conducted through metallographic inspection, SEM combined with EDS, XRD and Vickers microhardness in each case.

To prepare the specimens for metallographic and SEM analysis, precise cutting then grinding were carried out using progressively

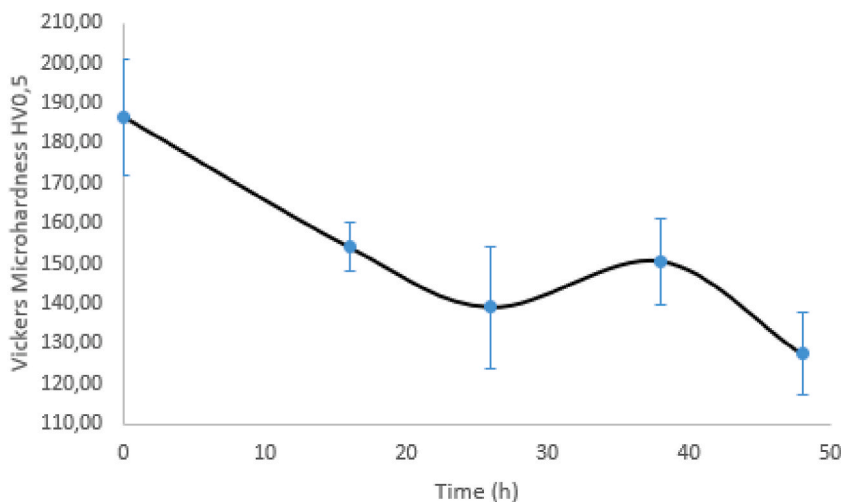


Fig. 9. Vickers microhardness HV0.5 testing results.

finer abrasives, namely 240P, 320P, 600P, 800P and 1200P. Subsequently, the specimens underwent polishing on 6  $\mu\text{m}$  and 1  $\mu\text{m}$  diamond pads with diamond solutions. The chemical etching was done by HF for a duration of 2–3s.

In the case of XRD and Vickers microhardness specimens, they underwent grinding and polishing using the same aforementioned procedure. Vickers microhardness testing was done by a 10g mass and dwell time of 10s, and 7 was the number of measurements for each specimen. The scanning rate during XRD analysis was at 4°/min and the 2 $\theta$  scan covered a range from 5° to 90°. The experimental measurements were conducted using a Bruker XRD machine.

### 3. Results and discussion

#### 3.1. As-cast alloy characterization

The as-cast alloy is characterized by thermal analysis of the cooled sample and dilatometry techniques (Figs. 2 and 3). Analysis of the cooling curve derivative revealed a distinct minimum peak corresponding to the solidus temperature which was found approximately 625 °C. The liquidus temperature corresponds to the temperature that has a derivative equal to 0 where a small isotherm appears and it has a value of 650 °C to the first. The cooling curve of the alloy is illustrated in Fig. 5.

The dilatometry analysis gave the curve of dilatation in the function of temperature, as shown in Fig. 6. Significant shifts in the thermal expansion coefficient were observed at temperatures of 250 °C, 400 °C and 515 °C. These transitions (highlighted in red circles in Fig. 6) are attributed to phase transformations in the alloy which play a crucial role in dictating its mechanical properties. Notably, the prominent change in the thermal coefficient at 515 °C is of particular significance because it's the closest curve inflection to the solidus point. Based on the last result, the homogenization heat treatment temperature was chosen as 515 °C.

#### 3.2. Homogenization heat treatment investigation

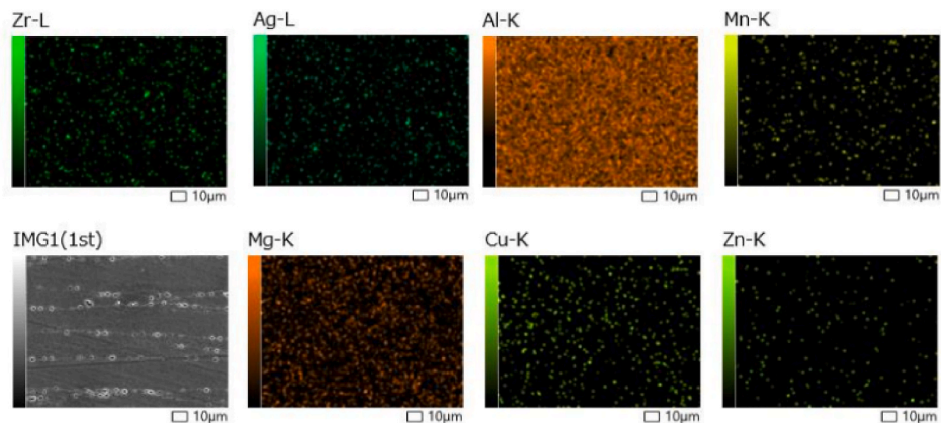
##### 3.2.1. Optical microscope images, SEM images and Vickers microhardness

The metallographic images of the homogenized samples are shown in Fig. 7(a–e). No dendritic structure was observed in any of the homogenized samples. Dark dots basically representing precipitates were prominently present at the grain boundaries. The grain boundaries are noticeable in all homogenization samples except the last one in Fig. 7(e), which presents 48h of homogenization heat treatment. The last sample has coarsened grains and hardly the grain boundaries are sighted.

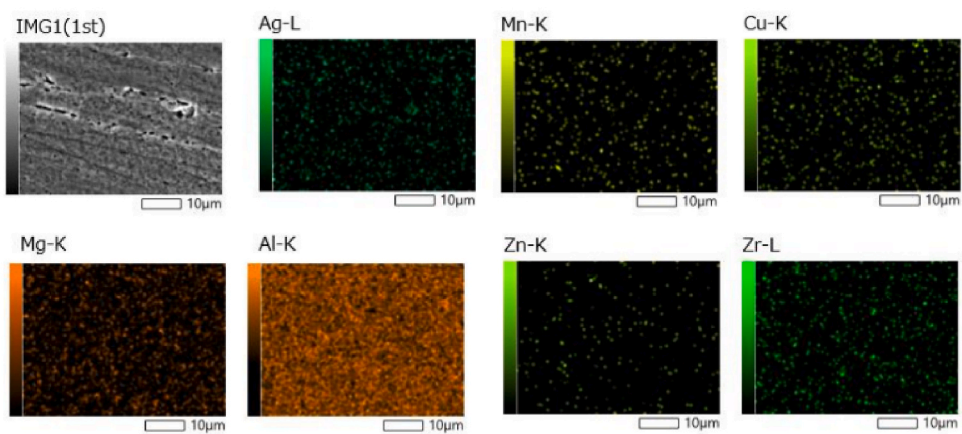
SEM images shown in Fig. 8(a–e) provide further insights into the evolution of grain boundaries precipitates with varying homogenization times. After 26 h h of heat treatment, the size of the precipitates is minimal as shown in Fig. 8(c). The size of the precipitates decreases from the as-cast till the 26h homogenization heat treatment sample and it increases until what appeared as the dissolution of those precipitates in the 48h sample as shown in the last image of SEM in Fig. 8(e), where the grain boundaries are hardly visible. Those findings are close to the results of Amichi and Bourahla [19] where the last homogenized sample of nearly the same Al–Li alloy for 24h at 530 °C has coarsened grains with no grain boundaries precipitates. Vickers microhardness results are illustrated in Fig. 9 where the as-cast alloy has an approximate value of 186 HV0.5. Ghosh et al. [20] found that the as-cast alloy has a hardness value of 165 HV10.

The microhardness plotted curve shows a local minimum hardness value after 26h heat treatment which coincides with the minimal size of the grain boundaries precipitates. As the grain boundaries precipitate size increased, the microhardness value also increased. The last case (after 48h of heat treatment) exhibited the lowest microhardness value. The SEM and optical images can explain it as they show no precipitates at the grain boundaries, indicating precipitates dissolution and coarsened grains. This

(a)



(b)



(c)

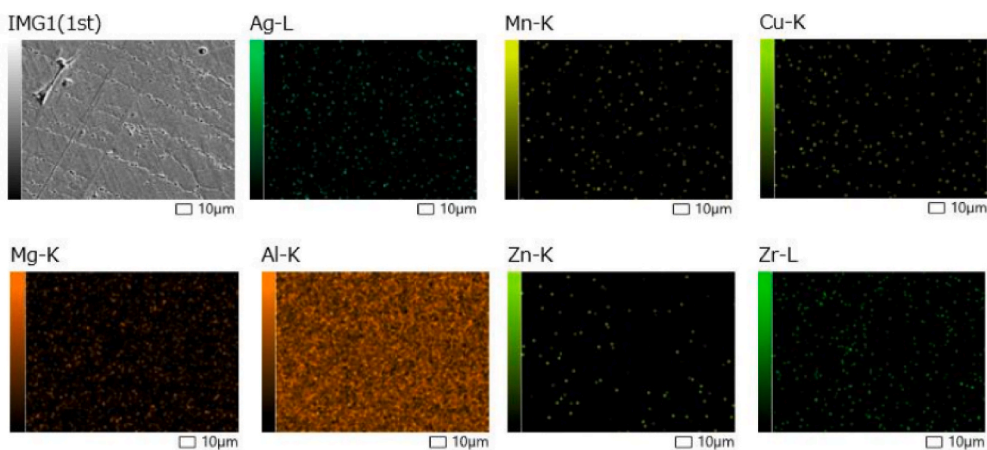


Fig. 10. EDS analysis, (a) 0h ref, (b) 16h, (c) 26h, (d) 38h, (e) 48h.

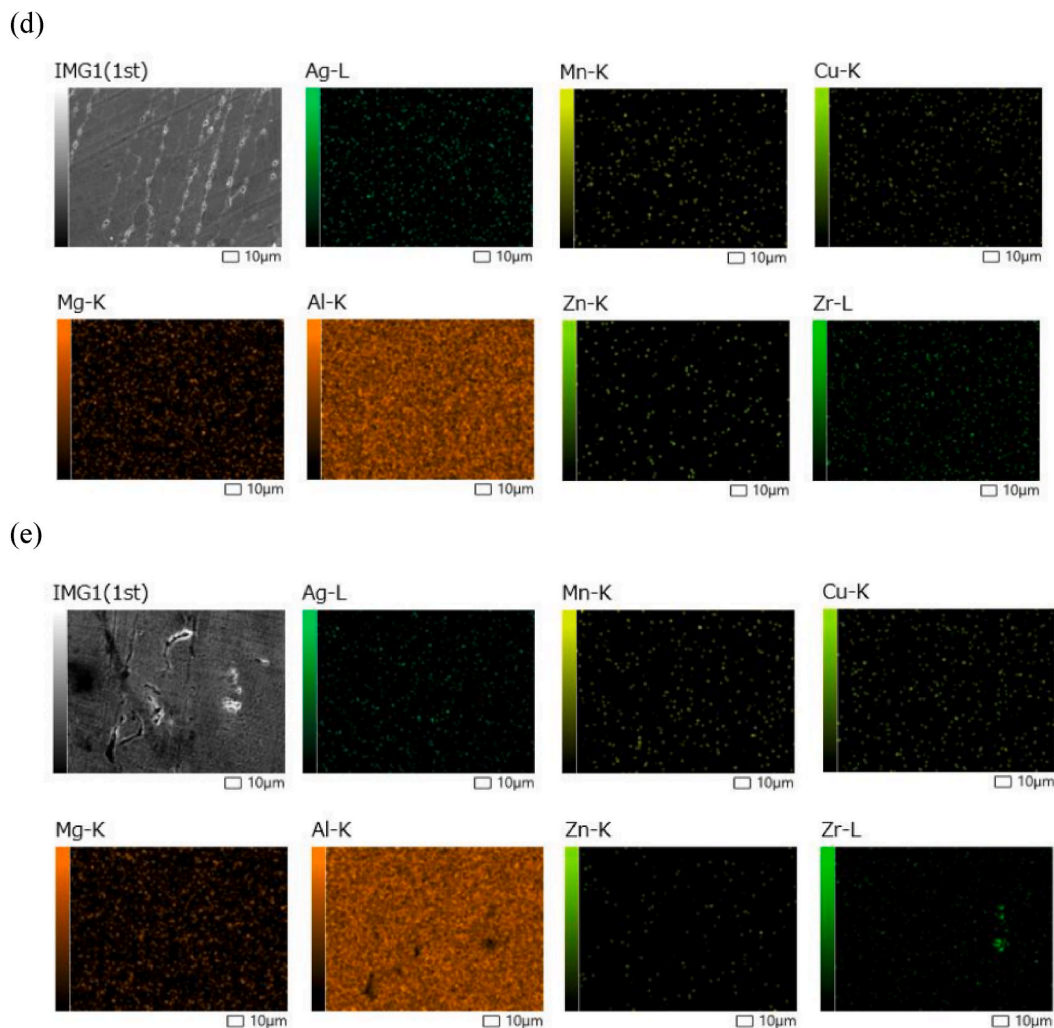


Fig. 10. (continued).

phenomenon aligns with the findings of Rezaei et al. [12] who investigated two Al–Li alloys with Al–3Cu–1(2)Li–0.1Zr chemical composition and found a fluctuation in hardness depending on the homogenization time at a constant temperature of 500 °C.

### 3.2.2. EDS analysis and XRD patterns

EDS analysis is presented in Fig. 10(a–e) as a surface mapping of each homogenized sample, which revealed the absence of dendritic segregation in EDS mapping in all the homogenized samples. The homogenized sample for 48h EDS in Fig. 10(e) showed minor segregation of Zr, which is responsible for the formation of  $\beta'$  precipitate. After 48h of homogenization heat treatment, the grain boundaries are coarse, suggesting the dissolution of  $\beta'$  precipitates which are responsible for grain boundary pinning.

XRD analysis, illustrated in Fig. 11(a–e), displayed the presence of the aluminum  $\alpha$  phase,  $\delta'$ ,  $\delta$  and  $\beta'$  precipitates. The  $\delta$ (AlLi) phase disappeared after 26h of homogenization, leaving behind the remaining precipitates of  $\delta$ ,  $\beta'$ . The  $T_1$  phase is not spotted in the XRD patterns as it should appear after the age hardening heat treatment. It's worth mentioning that the formed precipitates in this study are not the aging hardening precipitates responsible for the strengthening of the alloy. A Previous study conducted by Amichi and Bourahla [19] investigated an alloy with proximate chemical composition and found that the as-cast alloy exhibits the precipitates  $\beta'$  and  $\theta$ . Chen et al. [21] found in AA2196 alloy AlLi,  $Al_3Li$ ,  $Al_2Cu$  and  $Al_2CuLi$  phases in the as-cast state. However, after a homogenization heat treatment at 500 °C for 24h, only the  $Al_3Li$  phase remained. Wei et al. [11] found only  $\theta$  precipitates after subjecting an alloy with a composition of 2.65 % Cu, 1.47 % Li, 0.33 % Mn, 0.27%Mg and 0.12 % Zr (wt. %) to a heat treatment of 530 °C for 24h. The differences in the precipitates for each alloy are due mainly to the composition of the alloy; it differs when %Cu < %Li from the opposite case.

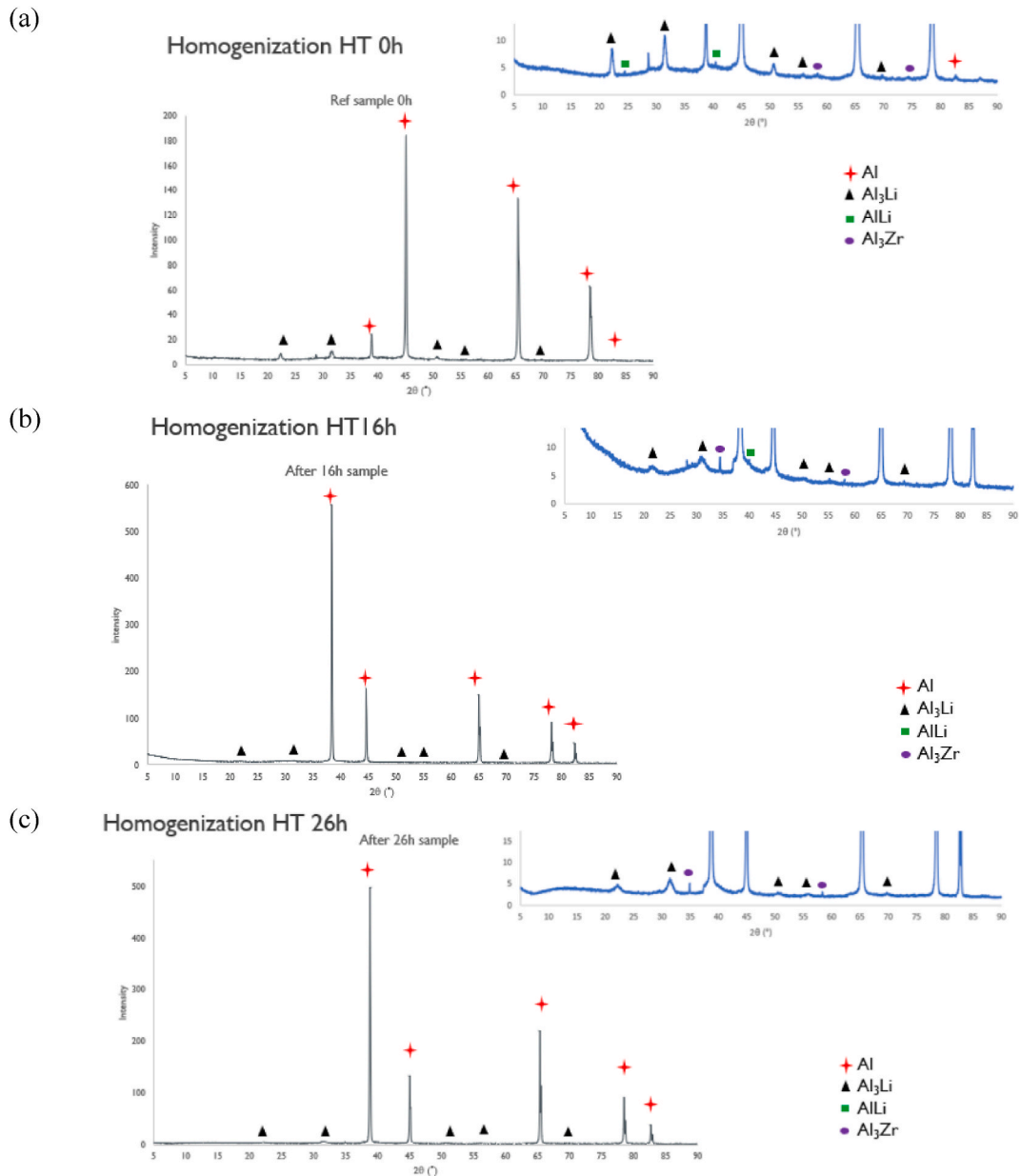


Fig. 11. XRD patterns, (a) 0h ref, (b) 16h, (c) 26h, (d) 38h and (e) 48h.

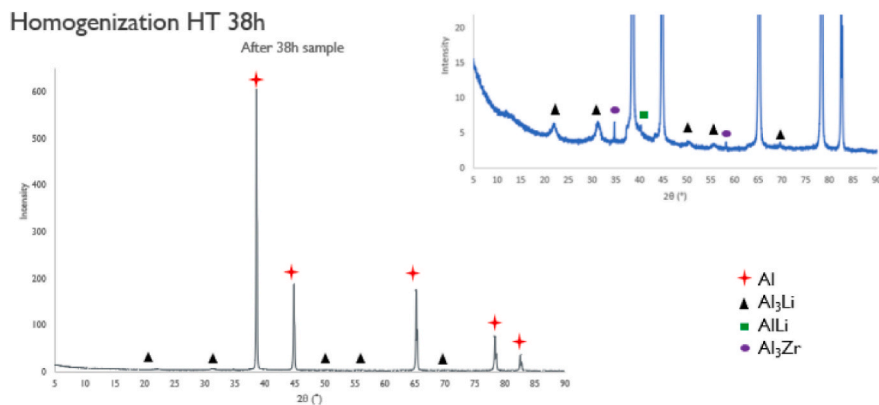
#### 4. Conclusion

This study investigates the as-cast alloy and the effects of homogenization heat treatment on an Al–Li–Cu–Mg–Zr alloy. Through thermal analysis, dilatometry, metallography, SEM/EDS, XRD and Vickers microhardness testing, comprehensive insights were gained regarding the alloy's thermal behavior, microstructural evolution, precipitates formation and mechanical properties.

The as-cast alloy was characterized using cooling curve thermal analysis and thermal expansion via dilatometry. The first technique gave the solidus temperature of the alloy as 625 °C and the temperature of liquidus was 650 °C phase. The second technique revealed the fluctuation in unidirectional deformation at 200 °C, 45 °C and 515 °C. Based on these findings and on that 515 °C temperature corresponds to the closest inflection point to the solidus temperature, the optimal temperature for the subsequent homogenization heat treatment was chosen as 515 °C.

During the homogenization in investigation, optical microscopy and SEM examinations demonstrated the absence of dendritic structure and the presence of grain boundaries precipitates. The size of those precipitated was minimal after 26h of heat treatment,

(d)



(e)

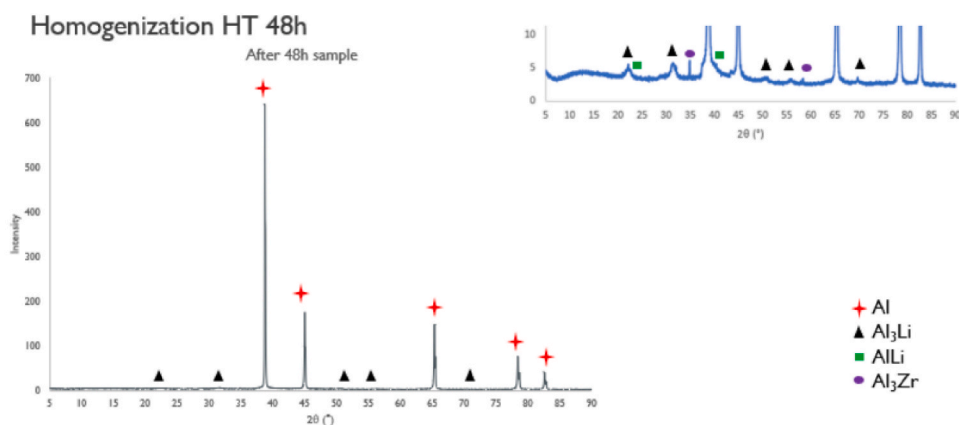


Fig. 11. (continued).

coinciding with a local minimum in Vickers microhardness value. EDS analysis confirmed the absence of dendritic segregation, while XRD patterns identified the presence of aluminum  $\alpha$  phase  $\delta'$ ,  $\delta$  and  $\beta'$  precipitates. The dissolution of  $\beta'$  precipitates was observed after 48h of homogenization heat treatment with coarsened grains. Based on all the findings of this work, the best homogenization time is 26h as a process preceding rolling.

#### Data availability statement

The raw/processed data required to reproduce the above findings cannot be shared at this time as the data also forms part of an ongoing study.

#### Additional information

No additional information is available for this paper.

#### CRediT authorship contribution statement

**Abdellah Lahbari:** Writing - original draft, Data curation, Conceptualization. **Kenza Bouchaala:** Writing - review & editing, Supervision, Methodology. **Hamza Essoussi:** Resources, Conceptualization. **Mustapha Faqir:** Project administration. **Said Ettaqi:** Investigation.

#### Declaration of competing interest

The authors declare that they have no known competing financial interests or personal relationships that could have appeared to influence the work reported in this paper.

## Acknowledgments

We thank Professor Badia Ait El Haj (ENSAM Meknes, Moulay Ismail University) for providing help in conducting computer-aided cooling curve analysis experiments.

## References

- [1] R.J. Rioja, Fabrication methods to manufacture isotropic Al-Li alloys and products for space and aerospace applications, *Mater. Sci. Eng., A* 257 (1) (1998) 100–107.
- [2] R.J.H. Wanhill, Aerospace applications of aluminum–lithium alloys, in: *Aluminum-lithium Alloys*, Butterworth-Heinemann, 2014, pp. 503–535.
- [3] H.S. Lee, J.H. Yoon, J.T. Yoo, Manufacturing Titanium and Al-Li alloy Cryogenic tanks, *Key Eng. Mater.* 837 (2020) 64–68.
- [4] Y. Wang, G. Zhao, Hot extrusion processing of Al–Li alloy profiles and related issues: a review, *Chin. J. Mech. Eng.* 33 (1) (2020) 1–24.
- [5] R.J. Rioja, J. Liu, The evolution of Al-Li base products for aerospace and space applications, *Metall. Mater. Trans.* 43 (9) (2012) 3325–3337.
- [6] E.N. Kablov, V.V. Antipov, J.S. Oglodkova, M.S. Oglodkov, Development and application prospects of aluminum–lithium alloys in aircraft and space technology, *Metallurgist* 65 (1–2) (2021) 72–81.
- [7] A. Abd El-Aty, Y. Xu, X. Guo, S.H. Zhang, Y. Ma, D. Chen, Strengthening mechanisms, deformation behavior, and anisotropic mechanical properties of Al-Li alloys: a review, *J. Adv. Res.* 10 (2018) 49–67.
- [8] H. Li, Y. Tang, Z. Zeng, Z. Zheng, F. Zheng, Effect of ageing time on strength and microstructures of an Al–Cu–Li–Zn–Mg–Mn–Zr alloy, *Mater. Sci. Eng., A* 498 (1–2) (2008) 314–320.
- [9] E.A. Hajjoui, K. Bouchaala, M. Faqir, E. Essadiqi, A Review of Manufacturing Processes, Mechanical Properties and Precipitations for Aluminum Lithium Alloys Used in Aeronautic Applications, *Heliyon*, 2022.
- [10] B. Rinderer, The metallurgy of homogenisation, *Mater. Sci. Forum* 693 (2011, September) 264–275. Trans Tech Publications Ltd.
- [11] X.Y. Wei, Z.Q. Zheng, Q.N. Chen, X. Fu, Homogenization treatment of an Al-Li-Cu-Mg-Mn-Zr alloy, *Mater. Sci. Forum* 546 (2007, June) 719–722. Trans Tech Publications Ltd.
- [12] A. Rezaei, S. Ahmadi, A. Shokuhfar, I. Foroutan, Investigation of homogenization treatment in Al-Li-Cu-Zr alloys, *Defect Diffusion Forum* 273 (2008, January) 536–541. Trans Tech Publications Ltd.
- [13] F. Zhang, J. Shen, X.D. Yan, J.L. Sun, X.L. Sun, Y. Yang, Homogenization heat treatment of 2099 Al–Li alloy, *Rare Met.* 33 (2014) 28–36.
- [14] H. Huang, W. Xiong, Z. Jiang, J. Zhang, A quasi in-situ study on the microstructural evolution of 2195 Al-Cu-Li alloy during homogenization, *Materials* 15 (19) (2022) 6573.
- [15] Chaoyang Li, Guangjie Huang, Lingfei Cao, et al., Effect of two-stage homogenization heat treatment on microstructure and mechanical properties of aa2060 alloy, *Crystals* 11 (1) (2020) 40.
- [16] Y. Shengli, S. Jian, Y. Xiaodong, L. Xiwu, Z. Fei, S. Baoqing, Homogenization treatment parameter optimization and microstructural evolution of Al-Cu-Li alloy, *Rare Met. Mater. Eng.* 46 (1) (2017) 28–34.
- [17] V. Singh, A.A. Gokhale, Melting and casting of aluminum–lithium alloys, in: *Aluminum-lithium Alloys*, Butterworth-Heinemann, 2014, pp. 167–185.
- [18] N. Akhtar, W. Akhtar, S.J. Wu, Melting and casting of lithium containing aluminium alloys, *Int. J. Cast Metals Res.* 28 (1) (2015) 1–8.
- [19] Amichi, R., & Bourahla, S. X RAYS analysis of microstructure in al-li alloys. *Chemtech*'15, 106..
- [20] K.S. Ghosh, K. Das, U.K. Chatterjee, Studies of microstructural changes upon retrogression and reaging (RRA) treatment to 8090 Al–Li–Cu–Mg–Zr alloy, *Mater. Sci. Technol.* 20 (7) (2004) 825–834.
- [21] X. Chen, X. Ma, H. Xi, G. Zhao, Y. Wang, X. Xu, Effects of heat treatment on the microstructure and mechanical properties of extruded 2196 Al-Cu-Li alloy, *Mater. Des.* 192 (2020) 108746.